Chapter 10

Brownian motors

10.1 Introduction

Directed transport in a spatiaIly periodic system in contact with a noise-generating thermal heat bath is ruled out by the second law of thermodynamics. The system has therefore to be driven away from thermal equilibrium by an additional deterministic or stochastic perturbation. PhysicalIy such a perturbation may be either externaIly imposed or of system-intrinsic origin, e.g. due to a second thermal heat reservoir at a different temperature or a non-thermal bath.

Besides the breaking of thermal equilibrium, a further requirement for directed transport in spatially periodic systems is c1early the breaking of the spatial inversion symmetry. The most cornmon situation typicaIly involves some kind of periodic and asymmetric, so-called *ratchet* (ratchet - spärrhake, tandat spärrhjul) potential.

It turns out that the breaking of thermal equilibrium and of spatial inversion symmetry are genericaIly sufficient for tbe occurrence of the so-called *ratchet effect*, i.e. the emergence of directed transport in a spatiaIly periodic system.

Progress in the field of Brownian motors has evolved tbrough contributions from rather different directions. One root of Brownian motor theory is the research on intracellular transport, specifically the biochemistry of molecular motors and molecular pumps. On the physical side, a ratchet effect in the form of voltage rectification by a DC-SQUID in the presence of a magnetic field and an unbiased AC-current has been experimentally observed.

10.2 Swimming bacteria.

Adopted from H. Berg Physics Today Jan. 24 (2000).

Escherichia coli is a single-celled organism that lives in our guts. It is equipped with a set of rotary motors only 45 nm in diameter. Each motor drives a long, thin, helical filament that extends several cell body lengths out into the external medium. The assemblage of motor and filament is called a *flagellum*. The concerted motion of several flagella enables a cell to swim. A cell can move toward regions that it deems more favorable by measuring changes in the concentrations of certain chemicals in its environment (mostly nutrients), deciding whether life is getting better or worse, and then modulating

the direction of rotation of its flagella. Thus, in addition to rotary engines and propellers, *E. colis* standard accessories include particle counters, rate meters, and gear boxes. This microorganism is an advanced nanotechnology device, and some of its features from the perspectives of chemistry, and physics will be discussed.

E. coli and *Salmonella typhimurium*, two closely related organisms, are the principal subjects of work being done on bacterial chemotaxis (the motion of bacteria toward chemical attractants or away from chemical repellents). That work has yielded an important model for understanding the behavior of cells at the molecular level.

One of the first to study the motion of bacteria was Antony van Leeuwenhoek. He used a single-lens microscope, and was intrigued by animalcules (little animals) that he saw in his well water. He wanted to know whether they might survive exposure to pepper, so he ground up some and added it to a sample. The number of animalcules waxed and waned until 6 August 1676, when he made a discovery:

> I now saw very plainly that these were little eels, or worms, lying all huddled up together and wriggling; just as if you saw, with the naked eye, a whole tubful of very little eels and water, with the eels a-squirming among one another: and the whole water seemed to be alive with these multifarious animalcules. This was for me, among all the marvels that I have discovered in nature, the most marvellous of all; and I must say, for my part, that no more pleasant sight has ever yet come before my eye than these many thousands of living creatures, seen all alive in a little drop of water, moving among one another, each several creature having its own proper motion.

He was looking at a spirillum, probably *Spirillum volutans*, the large bacterium shown in figure 10.1. Leeuwenhoek never saw its flagella. Those organelles of locomotion were first seen on *Chromatium okenii*, another large bacterium, by Christian Ehrenberg in 1836, and later on *S. volutans* by Ferdinand Cohn in 1872.

The subject of bacterial behavior was taken up systematically in the 1880s by the physiologist Theodor Engelmann in Utrecht, and by the botanist Wilhelm Pfeffer in Tübingen. They studied the responses of various species of bacteria to light, oxygen, salts, and a variety of nutrients. Pfeffer, who thought that bacteria could steer toward or away from a chemical source, coined the term chemotaxis to describe their attraction or repulsion. The role that flagella play in that response was examined in detail after dark-field condensers of high numerical aperture were developed, beginning in 1909 with work done by Karl Reichert and culminating in 1920 with the work of Paul Metzner, who described the motion of flagellar bundles of *S. volutans* in stunning detail.

S. volutans has two flagellar bundles (as shown in the figure), each composed of about 25 flagellar filaments. Here, the cell is swimming from left to right. Its body is helical. The bundle on the left is in the tail configuration; the one on the right is in the head configuration. When the filaments change their directions of rotation, the bundles switch their configurations and the cell moves in the opposite direction.

An *Escherichia coli* bacterium is shown below the *S. volutans* for comparison. As many as six flagellar filaments arise at random from the sides of the *E. coli* cell and form a bundle that appears near one pole. Rotation of the filaments in the bundle pushes the cell forward. When the bundle changes its orientation, the cell goes off in a new direction.

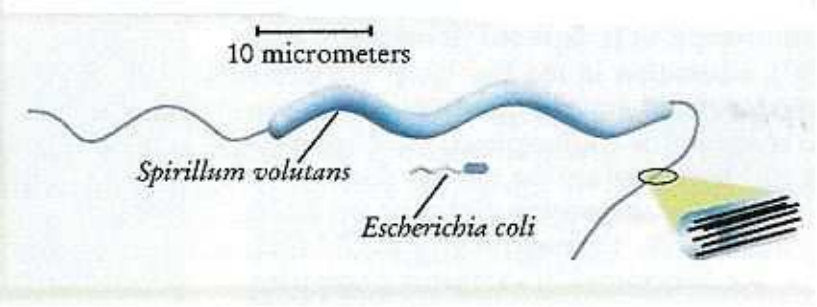

Figure 10.1: *Sketch of the bacteria* Spirillium volutans *and* Escherichia coli. *From Berg H. C. Physics Today Jan 24 (2000).*

10.3 Escherichia coli

Anatomy of *E. coli*

E. coli (like *S. typhimurium*) is a cylindrical organism with hemispherical endcaps (as figure 10.2 shows). The cell, which weighs only 1 picogram, is about 70% water. Some strains are flagellated and motile; others are nonflagellated and nonmotile. When motile cells are grown in a rich medium (such as salts plus a mixture of amino acids), they swim in the direction of their long axis at a rate of about 35 diameters per second, often changing course but rarely stopping.

The chromosome of *E. coli* consists of a single doublestranded chain of DNA about 700 times longer than the body of the cell. There are 4 639 221 base pairs specifying 4288 genes, most of which encode proteins. The functions of only about 60% of these proteins are known. About 50 different kinds of proteins are required to produce the cells chemotaxis, roughly half for the assembly of flagella and half for behavioral control.

When *E. coli* grows, it first gets longer and then divides in the middle. In a sense it is immortal, because the mother cell is replaced by two daughters, essentially identical to the daughters of the previous generation. The molecules of DNA in the members of a given set of descendants are identical except for mutations, which occur spontaneously for a given gene, at the rate of about 10^{-7} per generation.

If well fed and held at the temperature of the human gut (37° C), *E. coli* can synthesize and replicate everything it needs to make a new copy of itself in about 20 minutes. Thus, if we start at noon today with one cell (and lots of food), by noon tomorrow there will be $2^{72} = 4.7 \times 10^{21}$ cells – enough to pack a cube 17 meters on a side! This replication rate explains why single cells dispersed on the surface of hard nutrient agar soon become mounds of cells (colonies) a millimeter or so in diameter and why, in soft agar, the motile progeny of a single cell soon populate the entire plate.

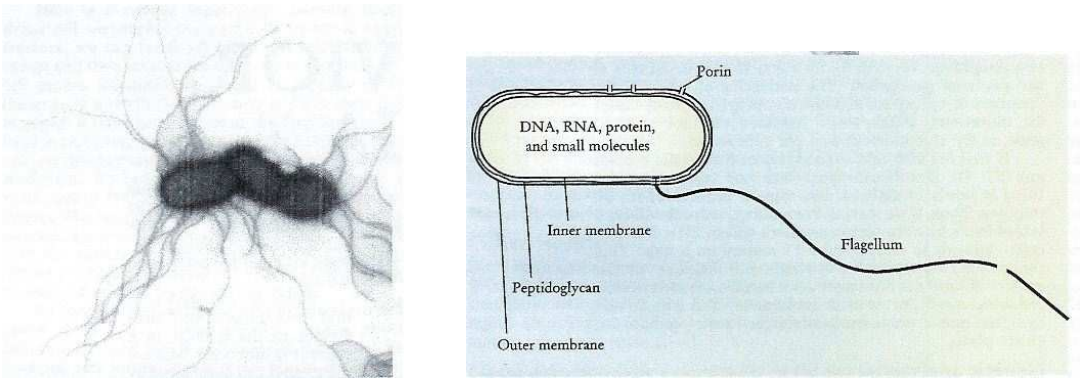

Figure 10.2: *Motile bacteria. Left: Three-cell cluster of* Salmonella typhimurium. *The cell bodies are about 1 μm in diameter and 2 μm long. The flagellar filaments have a wavelength of about 2.3 μm but are distorted by interactions with the substrate. The filaments are 23 nm thick. Right: Scale drawing of Escherichia coli, showing one flagellum, truncated, and three porins (protein channels that allow the entry of water-soluble nutrients). A typical cell has up to six flagella and hundreds of porins. The cell body is 2 μm long; the multilayered wall is about 30 nm thick. The outer membrane is made of polysaccharides and lipids, with the sugar chains pointing outward. The inner membrane's phospholipid bilayer core resembles the membranes that enclose human cells. This membrane is traversed by proteins involved in sensory transduction and in transporting materials and harvesting energy. It constitutes the main permeability barrier that enables the cell to retain the chemicals that make up the cytoplasm – DNA, RNA, proteins, and various water-soluble molecules of lower molecular weight. Between the inner and outer membranes is a porous, gauzelike layer of peptidoglycan (polysaccharide chains cross-linked by peptides), which gives the cell its rigidity and cylindrical shape. When the assembly of this polymer is blocked by an antibiotic such as penicillin, a growing cell cannot cope with the high osmotic pressure of its cytoplasm, and it blows up. The intermembrane space, the periplasm, contains a variety of proteins that either bind molecules that interest the cell (such as sugars) or destroy molecules that pose a threat (such as foreign DNA). From Berg H. C. Physics Today Jan 24 (2000).*

The flagellum

The flagellum is an organelle that has three parts (as figure 10.3 shows). There is a basal body consisting of a reversible rotary motor embedded in the cell wall, beginning within the cytoplasm and ending at the outer membrane. There is a short proximal hook, which is a flexible coupling or universal joint. And there is a long helical filament, which is a propeller.

Torque is generated between a stator connected to the rigid framework of the cell wall (to the peptidoglycan) and a rotor connected to the flagellar filament. The proteins MotA and MotB are thought to constitute the elements of the stator; FliF, G, M, and N (the MS and C rings) those of the rotor; FlgB, C, F, and G those of the drive shaft; and FlgH and I (the L and P rings) those of the bushing that guides the driveshaft out through the outer layers of the cell wall.

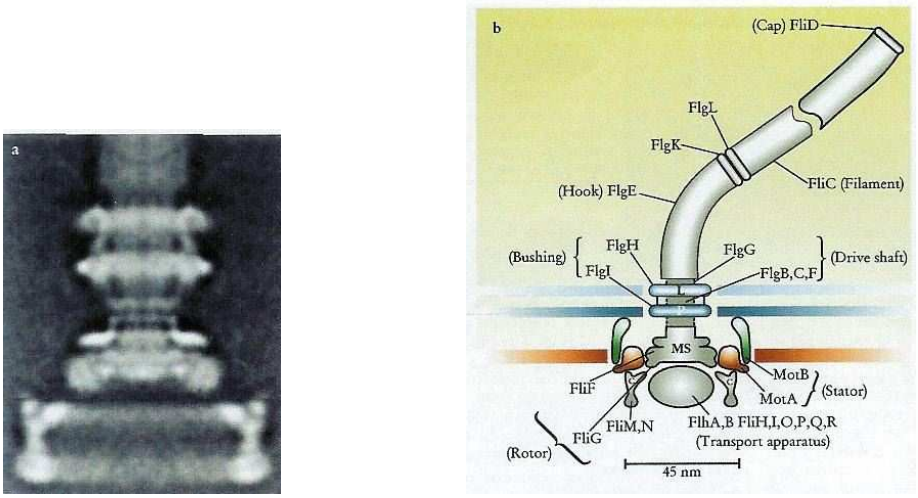

Figure 10.3: *Bacterial motor and drive train. (a) Rotationally averaged reconstruction of electron micrographs of purified hook-basal bodies. The rings seen in the image and labeled in the schematic diagram (b) are the L ring, P ring, MS ring, and C ring. From Berg H. C. Physics Today Jan 24 (2000).*

The proteins that make up the flagellum are present in multiple copies. For example, there are about 5000 molecules of FliC (also called flagellin) per helical turn of the filament, which can have as many as six turns. The MS, P, and L rings each contain about 26 copies of FliF, FlgI, and FlgH, respectively. There appear to be eight stator elements (complexes of MotA and MotB), each of which exerts a similar force.

If one fixes a wild-type cell to a glass slide by one of its flagellar filaments, the motor at the base of that filament spins the cell body at about 10 Hz. This technique is known as tethering. If one tethers a paralyzed cell, such as one with defective MotB, the cell body simply executes rotational Brownian movement, like a mirror on a galvanometer fiber. However, if wild-type MotB is made – for example, if a copy of a wild-type gene is added to the cell and expressed – then rotation resumes. The good MotB proteins that are made replace the bad ones, and the cell speeds up. Changes in speed are abrupt, generating a speed – time plot in the form of a staircase with eight steps of equal height.

The flagellum is assembled from the inside out, with the axial components exported through a central channel. The filament grows at the distal end, with molecules of FliC added under the distal cap, which is made of FliD. The growth process is subject to exquisite genetic control. FliC, for example, is not made until the assembly of the basal body is completed. When it is completed, the same apparatus that exports FliC pumps an inhibitor of late-gene transcription out of the cell. This removes the inhibition.

The motor is driven by protons flowing from the outside to the inside of the cell (except for marine bacteria and bacteria that live at high pH, where sodium ions are used instead). The source of energy is a transmembrane electrical potential or pH gradient (or both), generated by respiration for cells grown aerobically. MotA and MotB form a transmembrane channel. Proton translocation is thought to cause the cytoplasmic part of MotA to move or change its shape and exert a force on FliG, thereby driving the rotor.

Figure 10.4: *This plot shows about 30 s in the life of one Escherichia coli K-12 bacterium swimming in an isotropic homogenous medium.18 The track spans about 0.1 mm, left to right. The plot shows 26 runs and tumbles, the longest run (nearly vertical) lasting 3.6 s. The mean speed is about 21 mm/s. From Berg H. C. Physics Today Jan 24 (2000).*

In each cycle of this process, the rotor advances by one or more steps, which are of equal angular increment. From an analysis of fluctuations in the period of rotation (assuming exponentially distributed waiting times between steps), the number of steps is found to be at least 50 per revolution per stator element. As the number of stator elements increases toward eight, the rotation becomes smoother. The number of steps for the intact motor is at least 400 per revolution. Individual steps have yet to be resolved: They are filtered out by the elastic tether.

Detecting chemical gradients

The motor runs either clockwise (CW), as seen by an observer standing on the outside of the cell looking down at the hook, or counterclockwise (CCW), with protons continuing to flow from the outside to the inside of the cell. Switching direction involves the proteins FliG, M, and N.

In a cell wild type for chemotaxis, CW and CCW modes alternate (with exponentially distributed waiting times). When the motors turn CW, the flagellar filaments work independently, and the cell body moves erratically with little net displacement; the cell is then said to "tumble". When the motors turn CCW, the filaments rotate in parallel in a bundle that pushes the cell body steadily forward, and the cell is said to "run". The two modes alternate. The cell runs and tumbles, executing a three-dimensional random walk, as shown in figure 10.4.

When different flagellar motors in the same cell are studied under conditions in which they cannot interact mechanically, they change directions independently. Yet, when a flagellar bundle drives the cell forward, all of the motors have to rotate CCW. The events that bring about this coordination are not yet understood. The mean run interval is about 1 s, whereas the mean tumble interval is only about 0.1 s. Both of the times are exponentially distributed.

Although the change in angle generated by a tumble is approximately random, there is a slight forward bias. When, by chance, a cell moves up a spatial gradient of a chemical attractant or down a spatial gradient of a chemical repellent, runs are extended. When, by chance, it moves the other way, runs revert to the length observed in the absence of

a gradient. Thus, the bias in the random walk that enables cells to move up or down gradients is positive.

E. coli does not determine whether there is more attractant, say, in front than behind; rather, it determines whether the concentration increases when it moves in a particular direction. Studies of impulsive stimuli indicate that a cell compares the concentration observed over the past 1 s with the concentration observed over the previous 3 s and responds to the difference.

Constraints imposed by physics

Let's look again at the runs in figure 10.4. They are not quite straight. The cell is subject to rotational Brownian movement that causes it to wander off course by about 30° in 1 s. After about 10 s, it drifts off course by more than 90° and forgets the direction in which it was going. This makes earlier measurements irrelevant and sets an upper limit on the time that the cell has to decide whether life is getting better or worse. A lower limit is set by the time required for the cell to count enough molecules of attractant or repellent to determine their concentration with adequate precision. The number of receptors required for this task proves to be remarkably small, because diffusion of the molecules to be sensed enables them to be sampled by different points on the surface of the cell with great efficiency.

Flagellar mechanics is dominated by viscosity, not inertia: The Reynolds number is low, less than 10^{-4}. So flagella generate thrust by using viscous drag. The viscous drag on a thin rod is about twice as great when the rod moves sideways as when it moves lengthwise. As a result, when oriented slantwise and pulled downward through a viscous medium, a rod moves to one side. So, when a cell rotates a helical filament (in effect, a series of slantwise rods), it has to push as well as twist. In reaction the cell body translates and rolls. This scheme may not be very efficient, but it works!

10.4 The proteins Myosin and Kinesin walks by an hand-over-hand mechanism

Actin filaments form the "tracks" along which protein motors walk, thereby generating muscle contraction. Many other examples of walking motors are known in cells. Figure 10.5 shows a vesicle being dragged along a microtubule to its destination at an axon terminal. This axonal transport brings needed proteins to the axon terminal, as well as the ingredients from which synaptic vesicles will be built. A family of single-protein motors called kinesins supply the motive force for this and other motions, for example, the dragging of chromosomes to the two halves o a dividing cell. Indeed, selectively staining both the microtubules and the kinesin (by attaching fluorescent markers to each) shows that they are generally found together in the cell. It is even possible to follow the progress of individual kinesin molecules as they walk along individual microtubules. In such experiments, the kinesin molecules begin to walk as soon as a supply of ATP molecules is added; they stop when the ATP is used up or washed away. Other motors generate rotary motion. Examples include the motor that drives the bacterial flagellum discussed above, and the one that drives the synthesis of ATP in mitochondria. Rather than being driven directly by ATP, both of these motors use as their "fuel" a chemical

imbalance between the sides of the membrane they span. Ultimatdy, the imbalance comes from tire cell's metabolic activity.

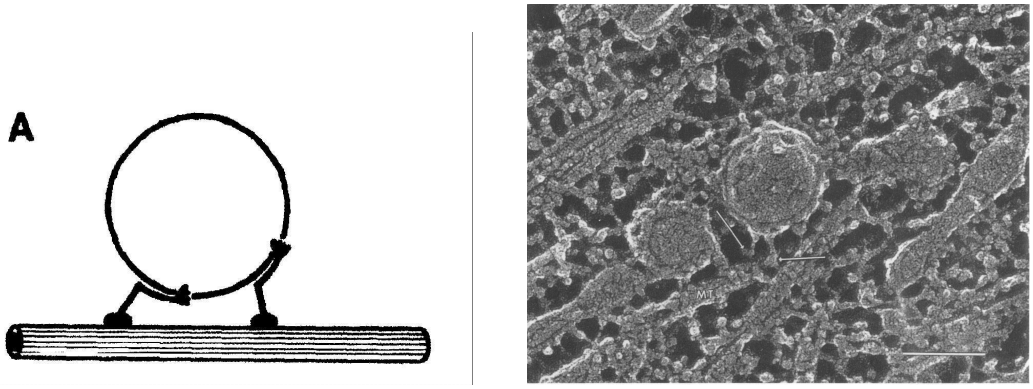

Figure 10.5: *Left: Model showing how kinesin drags a vesicle along a microtubule. Right: Micrograph appearing to show the situation sketched in left figure. Arrows show the attachments points. From Hirokawa, N. et. al Cell* **56** *867 (1989).*

Myosin

Myosin V is a cargo-carrying processive motor that takes 37-nm center of mass steps along actin filaments. Defects in this protein lead to immunological and neurological diseases. Like many other processive motors, it has two heads held together by a coiled-coil stalk (fig. 10.6). Each head of myosin V contains a catalytic domain responsible for actin binding and ATP hydrolysis and a light chainbinding domain that likely acts as a lever arm to amplify small nucleotide-dependent conformational changes in the catalytic domain.

How the two heads of myosin V are coordinated to produce steps is a central, partly unresolved question. Biochemical and biophysical studies suggest a hand-over-hand walking model in which the two heads alternate in the lead (fig. 10.6, left). Another possibility is the so-called inchworm model in which one head always leads (fig. 10.7, right).

The hand-over-hand and inchworm models make different, testable predictions for the motions of each individual head (fig. 10.6). For example, the inchworm model predicts that the step size of each catalytic domain is equal to the step size of the stalk [35 to 40 nm or 37 nm]. In contrast, the hand-over-hand model predicts that the trailing catalytic domain takes a step that is twice the step size of the stalk while the leading catalytic domain does not move. For a single fluorophore attached to the light chain domain of myosin V, the inchworm model predicts a uniform step size of 37 nm, whereas the hand-over-hand model predicts alternating steps of $37 - 2x, 37 + 2x$, where x is the in-plane distance of the dye from the midpoint of the myosin (fig. 10.6 and 10.7).

The conclusion from various experiments is that myosin V moves in a hand-over-hand fashion. Other tightly coupled motors, such as kinesin, seems to follow a similar scheme. Two types of hand-over-hand models have been proposed: an asymmetric model where each head is not functionally equivalent and where the stalk need not twist, and a symmetric model where each head is functionally equivalent and the stalk twists 180° on

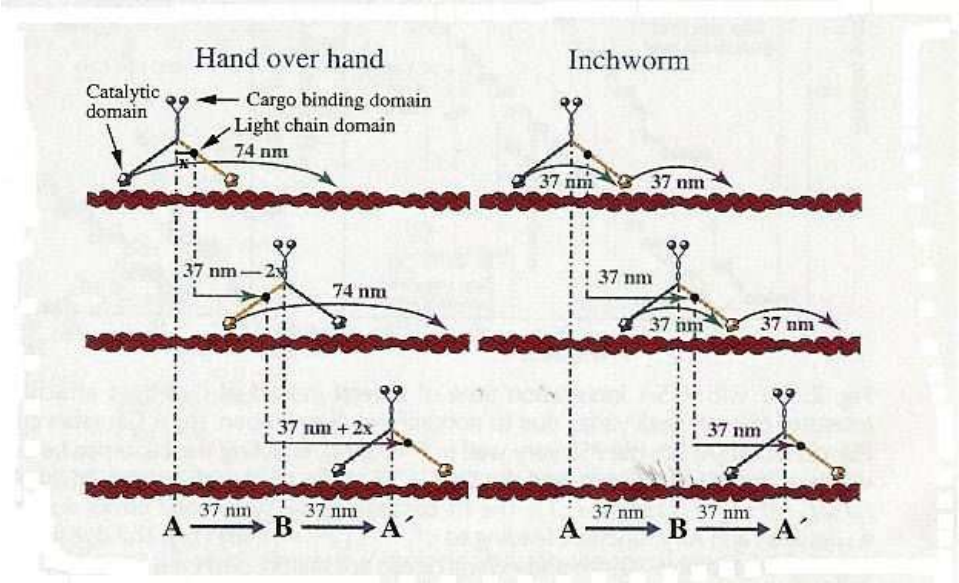

Figure 10.6: *Hand-over-hand versus inchworm model of myosin V motility. A calmodulin light chain is labeled with a single fluorescent dye and exchanged into the myosin V light chain domain, where it binds in one of several possible positions (black dot, schematic representation of dye position). In the hand-overhand model, the rear head moves 74-nm forward but the front head does not move, the stalk moves 37 nm, and the dye takes alternating* $37 \pm 2x$ *nm steps. (If the dye is a different distance from the stalk in the forward versus rear light chain domains, due to asymmetry in the myosin V structure, then* x *is the average distance of the dye from the stalk.) In the inchworm model, all parts of the myosin move 37-nm forward, and one head always leads. From Yildiz, A. et. al Science* **300** *2061 (2003)*

each step. It has been found that the coiled-coil stalk of kinesin does not systematically twist as the motor steps, a result also reported for myosin V. Such asymmetric hand-over-hand models are attractive for cargo-carrying motors because they do not require a twisting of a large cargo or, conversely, a large torque that would tend to twist the motor. A definitive conclusion, however, between a symmetric and asymmetric hand-over-hand mechanism for myosin V – and perhaps other biomolecular motors – will need to await further investigations.

Kinesin

Kinesin is a double-headed motor protein that moves along microtubules in 8-nanometer steps. Two broad classes of model have been invoked to explain kinesin movement as in Myosin: hand-over-hand and inchworm. By measuring the stepwise motion of individual enzymes,wefind that some kinesin molecules exhibit a marked alternation in the dwell times between sequential steps, causing these motors to limp along the microtubule. Limping implies that kinesin molecules strictly alternate between two different conformations as they step, indicative of an asymmetric, hand-over-hand mechanism.

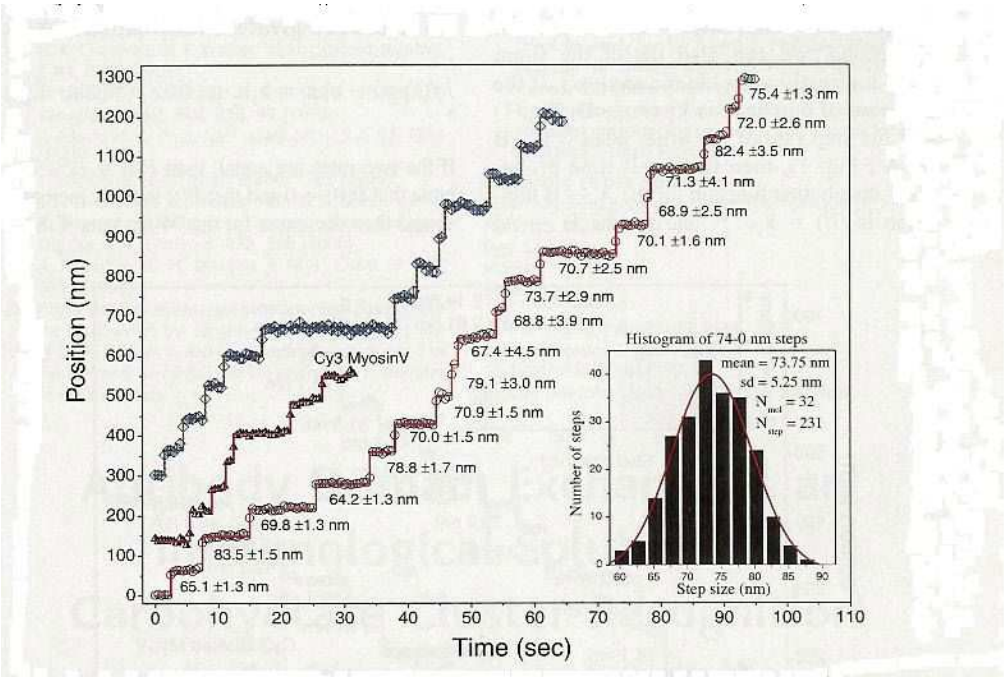

Figure 10.7: *Stepping traces of three different myosin V molecules displaying alternating steps, and histogram of a total of six myosin Vs taking 69 steps. These step sizes indicate that the dye is 2 to 3 nm from the center of mass along the direction of motion. The bottom right trace is for a Cy3-labeled myosin V, whereas the other two are for BR-labeled myosin Vs. Due to the 0.5-s time resolution of measurements, some steps are missed and yield 74-nm apparent steps, the sum of two steps. From Yildiz, A. et. al Science* **300** *2061 (2003)*

Results from a variety of single-molecule experiments have furnished insights into the mechanochemical properties of kinesin motor proteins. Individual kinesin dimers move processively, making discrete 8-nm steps at stochastic intervals, and may take a hundred or more steps before releasing from the microtubule surface. Processive motion persists even in the presence of sustained external loads up to several pN, suggesting that some portion of the kinesin dimer remains bound to the microtubule at all times. Kinesin molecules move on the microtubule surface lattice along paths parallel to the protofilaments, interacting with one binding site per tubulin dimer. Finally, kinesin moves in such a way as to hydrolyze exactly one adenosine triphosphate (ATP) molecule per 8-nm step. Two broad classes of stepping pattern are consistent with the foregoing observations: hand-over-hand models, in which the two heads step alternately, exchanging leading and trailing roles with each step, and inchworm models, in which a given head remains in the lead.

The active portion of the kinesin motor is formed from a dimer of identical heavy chains, which fold into twin heads attached to a single common stalk. The two globular heads, which carry enzymatic activity and bind ATP and microtubules, are joined to the stalk through short (13 amino acids) neck linker regions, consisting of single polypeptide chains. The heavy chains then intertwine to form a coiled-coil dimerization domain consisting of

classic heptad repeats. On the basis of this structure, free rotation (i.e., swiveling) of an individual head could occur, in principle, about the neck linker, but head motions would be summed mechanically at the point where the heavy chains merge into a common stalk, precluding further independent rotation beyond that point.

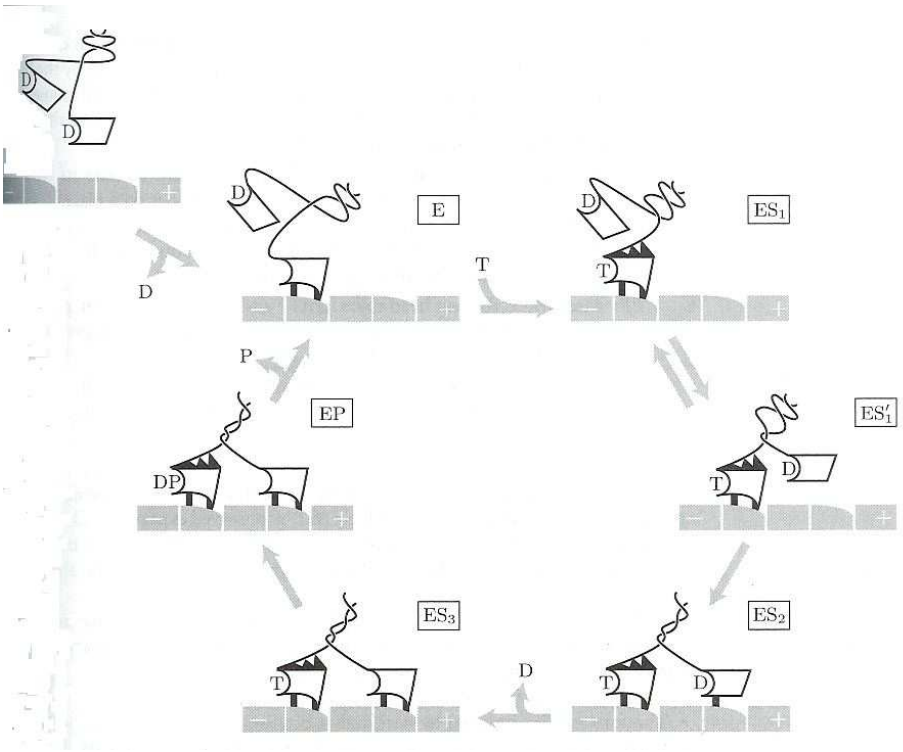

Figure 10.8: *Details of a model for kinesin stepping. Some elements of this mechanism are still under debate. The steps form a loop, to be read clockwise from upper left. The symbosl T, D and P denote ATP, ADP and inorganic phosphate respectively. The rapid isomerization step, ES_1, ES_1' is asumed to be nearly in equilibrium. From Nelson, P. Biological Physics, Energy, Information, Life.*

The proposed mechanism is summarized in figure 10.8. This cycle just shows some of the distinct steps in the enzymatic pathway. Initially (top left panel of the figure), a kinesin dimer approaches the microtobule from solution and binds on a head, releasing one of its ADP's.

E: This state shows the dimer with one head strongly bound to the microtubule.

ES_1, ES_1': The bound head binds an ATP molecule from solution. Its neck linker then docks onto its head, biasing the other head's random motion in the forward direction. There are also suggestions that the unbound head hops between the states ES_1 and ES_1'.

ES_2: The chain joining the two heads will have entropic elasticity. Being thrown forward and partially immobilized by the bound head's neck linker increases the probability

that the tethers will momentarily stretch far enough for the free head to reach the next binding site. It may bind weakly, then detach, many times.

ES_3: Eventually, instead of detaching, the forward head releases its ADP and binds strongly to the microtubule. Its stretched tether now places the whole complex under sustained strain. Both heads are now tightly bound to the microtubule, however, so the strain does not pull either one off.

EP: Meanwhile the rear head splits its ATP and releases the resulting phosphate. This reaction weakens its binding to the microtubule, and so it detaches.

E: The cycle is now ready to repeat, with the roles of the two heads reversed. The kinesin dimer has made one 8 nm step and hydrolyzed one ATP.

10.5 Basic concepts

Is it possible, and how is it possible to gain useful work out of unbiased random fluctuations? In the case of macroscopic fluctuations, the task can indeed be accomplished by various well-known types of mechanical and electrical rectifiers. Obvious daily-life examples are the wind-mill or the self-winding wristwatch. More subtle is the case of microscopic fluctuations, as demonstrated by the following Gedankenexperiment about converting Brownian motion into useful work. The basic idea can be traced back to a conference talk by Smoluchowski (1912), and was later popularized and extended in Feynman's Lectures on Physics, vol 1, chap. 46.

The main ingredient of Smoluchowski and Feynman's Gedankenexperiment is an axle with at one end paddles and at the other end a so-called ratchet, reminiscent of a circular saw with asymmetric saw-teeth. The whole device is surrounded by a gas at thermal equilibrium. So, if it could freely turn around, it would perform a rotatory Brownian motion due to random impacts of gas molecules on the paddles. The idea is now to rectify this unbiased random motion with the help of a *pawl* (spärrhake) (see fig. 10.9). It is indeed quite suggestive that the pawl will admit the saw-teeth to proceed into one "forward" direction but practically exclude a rotation in the opposite "backward" direction. Thus, it seems quite convincing that the whole gadget will perform on the average a systematic rotation in one direction, and this in fact even if a small load in the opposite direction is applied.

However, this naive expectation is wrong. In spite of the built in asymmetry, no preferential direction of motion is possible. Otherwise, such a gadget would represent a perpetuum mobile of the second kind, in contradiction to the second law of thermodynamics.

Since the impacts of the gas molecules take place on a microscopic scale, the pawl needs to be extremely small and soft in order to admit a rotation even in the forward direction. As Smoluchowski points out, the pawl itself is therefore also subjected to non-negligible random thermal fluctuations. So, every once in a while the pawl lifts itself up and the saw-teeth can freely travel underneath. Such an event clearly favors on the average a rotation in the "backward" direction. At overall thermal equilibrium a detailed quantitative analysis results in the subtle probabilistic balance which just ruIes out the functioning of such a perpetuum mobile.

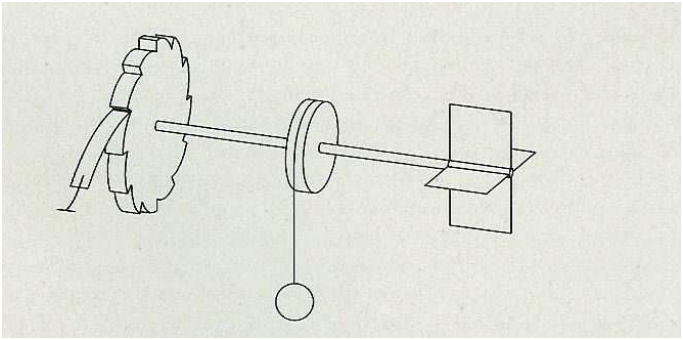

Figure 10.9: *Ratchet and pawl. The ratchet is connected by an axle with the paddles and with a spool, which may lift a load, In the absence of the pawl (leftmost object) and the load, the random collisions of the surrounding gas molecules with the paddles cause an unbiased rotatory Brownian motion. The pawl is supposed to rectify this motion so as to lift the load.*

Let's consider a Brownian particle in one dimension with coordinate $x(t)$ and mass m, which is moving in a periodic potential. Newton's equation of motion gives

$$m\ddot{x}(t) + V'(x(t)) = -\gamma\dot{x}(t) + \xi(t). \tag{10.1}$$

where $V(x)$ is a periodic potential with period L,

$$V(x + L) = V(x) \tag{10.2}$$

and broken spatial symmetry. A typical example is

$$V(x) = V_0 \left[\sin(kx) + A\sin(nkx)\right], \tag{10.3}$$

with $k = 2\pi/L$ and n an integer.

The left-hand side in (10.1) represents the deterministic, conservative part of the particle dynamics, while the right-hand side accounts for the effects of the thermal environment. These are energy dissipation, modeled in (10.1) as viscous friction with friction coefficient γ, and randomly ftuctuating forces in tbe form of tbe thermal noise $\xi(t)$.

The assumption that the environment is an equilibrium heat bath with temperature T and independent collisions implies that $\xi(t)$ is a Gaussian white noise of zero mean,

$$\xi(t) = 0, \tag{10.4}$$

and satisfying the fluctuation-dissipation theorem

$$\langle \xi(t)\xi(s) \rangle = 2\gamma k_{\mathrm{B}} T \delta(t - s),$$

For small systems the dynamics (10.1) is overdamped, and the inertia term $m\ddot{x}(t)$ may be neglected. We thus arrive at the equation

$$\gamma\dot{x}(t) = -V'(x(t)) + \xi(t). \tag{10.5}$$

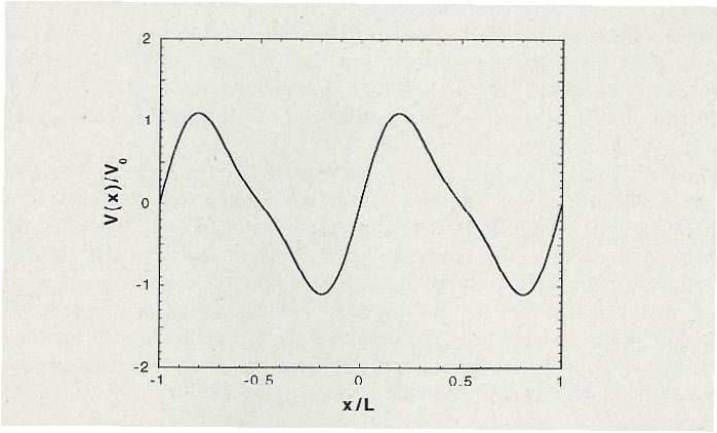

Figure 10.10: *Typical example of a ratchet-potential $V(x)$, periodic in space with period L and with broken spatial symmetry. Plotted is the example from (2.3) in dimensionless units.*

10.6 Fokker-Planck equation

We are interested in calculating the particle current $\langle \dot{x} \rangle$ in the presence of the potential $V(x)$.

A natural step is to consider a statistical ensemble of stochastic processes belonging to independent realizations of the random fluctuations $\xi(t)$. The corresponding probability density $P(x,t)$ describes the distribution of the Brownian particles and follows as an ensemble average of the form

$$P(x,t) = \langle \delta(x - x(t)) \rangle. \tag{10.6}$$

Then

$$\int_{-\infty}^{\infty} \mathrm{d}x \, P(x,t) = 1. \tag{10.7}$$

and $P(x,t) \geq O$ for all x and t.

The Fokker-Planck or Smoluchowski equation corresponding to (10.5) is

$$\frac{\partial}{\partial t} P(x,t) = \frac{\partial}{\partial x} \left\{ \frac{1}{\gamma} V'(x) P(x,t) + D \frac{\partial}{\partial x} P(x,t) \right\} \tag{10.8}$$

where $D = k_{\mathrm{B}} T / \gamma$.

The quantity of foremost interest in the context of transport in periodic systems is the particle current $\langle \dot{x}(t) \rangle$. ,

A direct average of (10.5) using (10.4) gives

$$\langle \dot{x}(t) \rangle = -\frac{1}{\gamma} \langle V'(x(t)) \rangle = -\frac{1}{\gamma} \int_{-\infty}^{\infty} \mathrm{d}x V'(x) P(x,t). \tag{10.9}$$

We can also derive an expression for $\langle \dot{x} \rangle$ from the Smoluchowski equation (10.8), which can be written as

$$\frac{\partial}{\partial t} P(x,t) + \frac{\partial}{\partial x} J(x,t) = 0, \tag{10.10}$$

with the probability current given by

$$J(x,t) = \langle \dot{x}(t)\delta(x - x(t))\rangle = \left\{ \frac{1}{\gamma} V'(x) + D\frac{\partial}{\partial x} \right\} P(x,t) \tag{10.11}$$

Integrating the probability current over x gives directly from the first equality above

$$\langle \dot{x}(t)\rangle = \int_{-\infty}^{\infty} \mathrm{d}x J(x,t) \tag{10.12}$$

and by a partial integration noting that $J(x = \pm\infty, t) = 0$ gives

$$\langle \dot{x}(t)\rangle = -\int_{-\infty}^{\infty} \mathrm{d}x x \frac{\partial}{\partial x} J(x,t) = \frac{\mathrm{d}}{\mathrm{d}t} \int_{-\infty}^{\infty} \mathrm{d}x x P(x,t)$$

which is an alternative definition of the particle current. Using the second equality in (10.11) in (**??**) and noting that $P(x = \pm\infty, t) = 0$ we recover the expression in (**??**)

Having established the evolution equation (10.8) governing the probability density $P(x,t)$ our next goal is to actually solve it and determine the current $\langle \dot{x}(t)\rangle$ according to (**??**).

We start by introducing the so-called reduced probability density and reduced probability current

$$\begin{aligned} \hat{P}(x,t) &= \sum_{n=-\infty}^{\infty} P(x + nL, t), \\ \hat{J}(x,t) &= \sum_{n=-\infty}^{\infty} J(x + nL, t). \end{aligned} \tag{10.13}$$

Then

$$\hat{P}(x + L, t) = \sum_{n=-\infty}^{\infty} P(x + (n+1)L, t) = \hat{P}(x,t),$$

and from the normailzation

$$\int_{-\infty}^{\infty} \mathrm{d}x P(x,t) = \sum_{n=-\infty}^{\infty} \int_{x_0+nL}^{x_0+(n+1)L} \mathrm{d}x P(x,t) = \sum_{n=-\infty}^{\infty} \int_{x_0}^{x_0+L} \mathrm{d}x P(x,t) = \int_{x_0}^{x_0+L} \mathrm{d}x \hat{P}(x,t) = 1$$

and similarly

$$\langle \dot{x}\rangle = \int_{x_0}^{x_0+L} \mathrm{d}x \hat{J}(x,t) \tag{10.14}$$

With $P(x,t)$ being a solution of the Fokker-Planck equation (10.8) it follows from the periodicity of $V(x)$ that also $P(x+nL,t)$ is a solution for any integer n. Since the Fokker-Planck equation is linear, it is also satisfied by the reduced density (10.13), and we have the continuity equation

$$\frac{\partial}{\partial t} \hat{P}(x,t) + \frac{\partial}{\partial x} \hat{J}(x,t) = 0, \tag{10.15}$$

with the explicit form of the reduced probability current

$$\hat{J}(x,t) = -\left\{ \frac{1}{\gamma} V'(x) + D\frac{\partial}{\partial x} \right\} \hat{P}(x,t) \tag{10.16}$$

In other words, as far as the particle current $\langle \dot{x} \rangle$ is concerned, it suffices to solve the Fokker-Planck equation with periodic boundary (and initial) conditions.

If we multiply both sides of (10.15) with x and integrate from x_0 to $x_0 + L$ we find

$$\begin{aligned} & \int_{x_0}^{x_0+L} \mathrm{d}x x \frac{\partial}{\partial t} \hat{P}(x,t) + \int_{x_0}^{x_0+L} \mathrm{d}x x \frac{\partial}{\partial x} \hat{J}(x,t) \\ = & \frac{\mathrm{d}}{\mathrm{d}t} \int_{x_0}^{x_0+L} \mathrm{d}x x \hat{P}(x,t) + \left[x \hat{J}(x,t) \right]_{x_0}^{x_0+L} - \int_{x_0}^{x_0+L} \mathrm{d}x \hat{J}(x,t) \\ = & \frac{\mathrm{d}}{\mathrm{d}t} \int_{x_0}^{x_0+L} \mathrm{d}x x \hat{P}(x,t) + L \hat{J}(x_0,t) - \int_{x_0}^{x_0+L} \mathrm{d}x \hat{J}(x,t) = 0 \end{aligned} \tag{10.17}$$

where x_0 is an arbitrary reference position. Then from (10.14) we find

$$\langle \dot{x} \rangle = \frac{\mathrm{d}}{\mathrm{d}t} \int_{x_0}^{x_0+L} \mathrm{d}x x \hat{P}(x,t) + L \hat{J}(x_0,t)$$

In other words, the total particle current $\langle \dot{x} \rangle$ is composed of the motion of the "center of mass" $\int_{x_0}^{x_0+L} \mathrm{d}x x \hat{P}(x,t)$ plus L times the reduced probability current $\hat{J}(x_0,t)$ at the reference point x_0. Especially, if the reduced dynamics assumes a steady state, characterized by $\mathrm{d}P(x,t)/\mathrm{d}t = 0$, then the reduced probability current $\hat{J}(x_0,t) = J^{\mathrm{st}}$ becomes independent of x_0 and t , and the particle current takes the form

$$\langle \dot{x} \rangle = L \hat{J}^{\mathrm{st}}$$

From (10.16) we then find

$$D \left[\beta V'(x) + \frac{\partial}{\partial x} \right] \hat{P}^{\mathrm{st}}(x) = D \mathrm{e}^{-\beta V(x)} \frac{\partial}{\partial x} \left[\mathrm{e}^{\beta V(x)} \hat{P}^{\mathrm{st}}(x) \right] = -\hat{J}^{\mathrm{st}}$$

or

$$\frac{\partial}{\partial x} \left[\mathrm{e}^{\beta V(x)} \hat{P}^{\mathrm{st}}(x) \right] = -\frac{1}{D} \mathrm{e}^{\beta V(x)} \hat{J}^{\mathrm{st}}$$

Integrating from x to $x + L$ gives

$$\mathrm{e}^{\beta V(x+L)} \hat{P}^{\mathrm{st}}(x+L) - \mathrm{e}^{\beta V(x)} \hat{P}^{\mathrm{st}}(x) = -\frac{\hat{J}^{\mathrm{st}}}{D} \int_x^{x+L} \mathrm{d}y \mathrm{e}^{\beta V(y)} \tag{10.18}$$

Since

$$V(x+L) = V(x), \quad \text{and} \quad \hat{P}^{\mathrm{st}}(x+L) = \hat{P}^{\mathrm{st}}(x)$$

the only solution to this equation is $\hat{J}^{\mathrm{st}} = 0$ and therefore

$$\frac{\partial}{\partial x} \left[\mathrm{e}^{\beta V(x)} \hat{P}^{\mathrm{st}}(x) \right] = 0$$

leading to

$$\hat{P}^{\mathrm{st}}(x) = \frac{1}{Z} \mathrm{e}^{-\beta V(x)}, \quad Z = \int_0^L \mathrm{d}y \mathrm{e}^{-\beta V(x)} \tag{10.19}$$

The steady state particle current must vanish

$$\langle \dot{x} \rangle = 0$$

It can be shown that the long-time asymptotic solution of a Fokker-Planck equation is unique.

Even though the absence of an average current is a simple consequence of the second law of thermodynamics, it is astonishing that in spite of the broken spatial symmetry there arises no systematic preferential motion of the random dynamics in one or the other direction.

10.7 Constant load

We now consider the ratchet in the presence of an additional homogeneous static force F:

$$\gamma\dot{x}(t) = -V'(x(t)) + F + \xi(t)$$

This scenario is one of the few exactly solvable cases.

We may incorporate the ratchet potential $V(x)$ and the force F into a single effective potential

$$V_{\text{eff}}(x) = V(x) - F$$

which is however no longer periodic.

For a negative force $F < 0$ the particle is pulled to the left, the effective potential will be tilted to the left as well. In view of $\langle\dot{x}\rangle = 0$ for $F = 0$ it is plausible that in such a potential the particles will move on the average downhill i.e. $\langle\dot{x}\rangle < 0$ for $F < 0$ and similarly $\langle\dot{x}\rangle > 0$ for $F > 0$.

Even if V_{eff} is no longer periodic the force V' is and therefore also $\hat{P}$. Replacing $V(x)$ with $V_{\text{eff}}(x)$ in (10.18) and using the fact that

$$V'(x + L) = V'(x)$$

or

$$V(x + L) - V(L) = V(x) - V(0), \quad V(x + L) - V(x) = V(L) - V(0)$$

gives

$$\hat{P}^{\text{st}}(x) = \frac{1}{Z}\frac{1}{D}\mathrm{e}^{-\beta V_{\text{eff}}(x)} \int_x^{x+L} \mathrm{d}y \mathrm{e}^{\beta V_{\text{eff}}(y)} \tag{10.20}$$

where

$$Z = \frac{1}{D}\int_0^L \mathrm{d}x \int_x^{x+L} \mathrm{d}y \mathrm{e}^{-\beta V_{\text{eff}}(y) - V_{\text{eff}}(x)} \tag{10.21}$$

This gives the stationary current

$$\langle\dot{x}\rangle = \frac{L}{Z}\left[1 - \mathrm{e}^{-\beta V_{\text{eff}}(L) - V_{\text{eff}}(0)}\right] \tag{10.22}$$

The first observation is that a time-independent probability density $\hat{P}^{\text{st}}(x)$ does not exclude a non-vanishing particle current $\langle\dot{x}\rangle$. The sign of this current agrees with the sign of F.

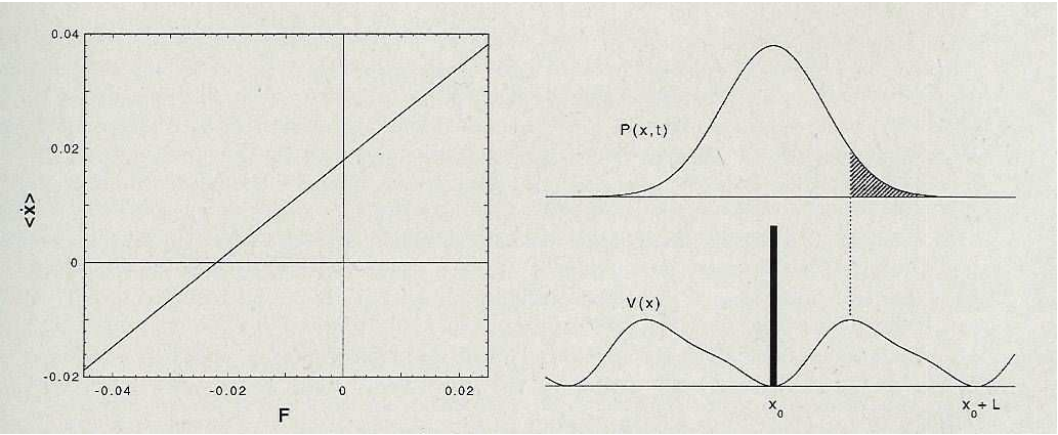

Figure 10.11: *Left figure shows average particle current* $\langle \dot{x} \rangle$ *versus force* F *for the temperature ratchet dynamics. The time- and ensemble-averaged current has been obtained by numericaIly evolving the Fokker-Planck equation (10.23) until transients have died out. The right figure shows the basic working mechanism of the temperature ratchet. Tbe figure illustrates how Brownian particles, initially concentrated at* x_0 *(lower panel), spread out when the temperature is switched to a very high value (upper panel). When the temperature jumps back to its initial low value, most particles get captured again in the basin of attraction of* x_0*, but aIso substantiaIly in that of* $x_0 + L$ *(hatcbed area). A net current of particles to the right, i.e.* $\langle \dot{x} \rangle > 0$ *results.*

10.8 Temperature ratchet

We now come to the central issue, namely the phenomenon of directed transport in a spatially periodic asymmetric system away from equilibrium.

As an obvious generalization of the loaded ratchet model we consider the case that the temperature of the Gaussian white noise $\xi(t)$ is subjected to periodic temporal variation with period τ, i.e.

$$\langle \xi(t)\xi(s) \rangle = 2\gamma k_{\mathrm{B}} T(t) \delta(t-s)$$

where

$$T(t) = T(t+\tau)$$

We can implement this into the Langevin equation by

$$\gamma \dot{x}(t) = -V'(x(t)) + F + g(t)\hat{\xi}(t)$$

where $\langle \hat{\xi}(t)\hat{\xi}(s) \rangle = 2\delta(t-s)$ and

$$g(t) = [\gamma k_{\mathrm{B}} T(t)]^{1/2}$$

As a choice for $T(t)$ we may take

$$T(t) = T_0 \left[1 + A \mathrm{sign}\left(2\pi t/\tau\right)\right]$$

The temperature thus jumps between $T(t) = T_0(1 + A)$ and $T(t) = T_0(1 - A)$ at every half period $\tau/2$.

Similarly as before we find the Fokker-Planck equation

$$\frac{\partial}{\partial t}\hat{P}(x,t) = \frac{\partial}{\partial x}\left\{\frac{1}{\gamma}(V'(x) - F)\hat{P}(x,t) + \frac{k_{\mathrm{B}}T(t)}{\gamma}\frac{\partial}{\partial x}\hat{P}(x,t)\right\} \tag{10.23}$$

Due to the permanent oscillations of $T(t)$ this equation does not admit a time-independent solution. Hence the reduced density $\hat{P}$ will not approach a steady state but rather a unique periodic behaviour in the long-time limit. It is therefore natural to include a time-average into the definition of $\langle \dot{x} \rangle$ as

$$\langle \dot{x}(t) \rangle = \frac{1}{\tau}\int_t^{t+\tau} \mathrm{d}t \int_0^L \mathrm{d}x \frac{F - V'(x)}{\gamma}\hat{P}(x,t). \tag{10.24}$$

The numerically calculated load curve in fig. 10.11 shows that $\langle \dot{x} \rangle > 0$ for an interval of negative F-values. Therefore the particles are climbing uphill on the average thereby performing work against the load force F.

A conversion of random fluctuations into useful work is called ratchet effect.

The basic working mechanism is the following. For high temperature the particles located at x_0 spread out. When the temperature jumps back to its initial low value most particles get captured again in the basin of attraction at x_0, but also substantially in that at $x_0 + L$. A net current of particles to the right with $\langle \dot{x} \rangle > 0$ results.

Certain enzymes (molecular motors) in living cells are able to travel along polymer filaments by hydrolyzing ATP (adenosine triphosphate). The interaction (chemical affinity) between the molecular motor and filament is spatially periodic and asymmetric, and thermal fluctuations play a significant role on these small scales.

On the crudest level hydrolyzoing an ATP molecule may be viewed as converting a certain amount of chemical energy into heat, thus we recover all the essential ingredients of a temperature ratchet. Such a temperature ratchet type model for intracellular transport may be acceptable as a primitive sketch of the basic physics.